

both speed the clearance and help restrict the spread of glutamate, first by binding and then transporting the transmitter (26).

REFERENCES AND NOTES

- J. D. Rothstein *et al.*, *Neuron* **13**, 713 (1994); K. Yamada *et al.*, *Neuroreport* **7**, 2013 (1996); Y. Kanai, P. G. Bhide, M. DiFiglia, M. A. Hediger, *ibid.* **6**, 2357 (1995).
- M. Takahashi, M. Sarantis, D. Attwell, *J. Physiol.* **497**, 523 (1996); Y. Kataoka and H. Ohmori, *J. Neurophysiol.* **76**, 1870 (1996).
- G. B. Grant and J. E. Dowling, *J. Neurosci.* **15**, 3852 (1995); S. A. Picaud, H. P. Larsson, G. B. Grant, H. Lecar, F. S. Werblin, *J. Neurophysiol.* **74**, 1760 (1995); B. Billups, D. Rossi, D. Attwell, *J. Neurosci.* **16**, 6722 (1996).
- S. Eliasof and C. E. Jahr, *Proc. Natl. Acad. Sci. U.S.A.* **93**, 4153 (1996).
- W. A. Fairman, R. J. Vandenberg, J. L. Arriza, M. P. Kavanaugh, S. G. Amara, *Nature* **375**, 599 (1995).
- J. I. Wadiche, S. G. Amara, M. P. Kavanaugh, *Neuron* **15**, 721 (1995).
- J. L. Arriza, S. Eliasof, M. P. Kavanaugh, S. G. Amara, *Proc. Natl. Acad. Sci. U.S.A.* **94**, 4155 (1997).
- A. Konnerth, I. Llano, C. M. Armstrong, *ibid.* **87**, 2262 (1990); D. J. Perkel, S. Hestrin, P. Sah, R. A. Nicoll, *Proc. R. Soc. London Ser. B* **241**, 116 (1990). Whole-cell recordings were made with infrared differential interference contrast optics at 22° to 24°C from PCs in 300- μ M-thick cerebellar slices prepared from 12- to 20-day-old rats. Pipettes had resistances of 0.9 to 1.2 megohm; at the end of 34/49 recordings, R_{series} (4.8 ± 0.3 megohm; range: 2.5 to 10.9 megohm, $n = 34$) was determined by measuring instantaneous current in response to 5-mV steps with only the pipette capacitance canceled. R_{series} was compensated >80%. The extracellular solution contained 119 mM NaCl, 2.5 mM KCl, 2.5 mM CaCl₂, 1.3 mM MgCl₂, 1 mM NaH₂PO₄, 26.2 mM NaHCO₃, 11 mM glucose, and 0.1 mM picrotoxin saturated with 95% O₂-5% CO₂. Pipette solutions contained 130 mM (K⁺ or Cs⁺) A⁻, 20 mM Hepes, 10 mM KCl or tetraethylammonium (TEA) chloride, 10 mM EGTA, and 1 mM MgCl₂, titrated to pH 7.3 with either CsOH or KOH; A⁻ denotes that NO₃⁻, SCN⁻, gluconate⁻ or Cl⁻, and KCl or TEA chloride was included in the K⁺- or Cs⁺-based solutions, respectively. Stimuli (10 to 100 V, 10 to 100 μ s, 0.067 to 0.1 Hz) were delivered by means of a patch pipette filled with bath solution. Signals were filtered at 1 or 2 kHz (EPSCs) and digitized at 5 to 10 kHz. Membrane potential values have been corrected for junction potentials. Reported values are the mean \pm SEM.
- J. Ferkany and J. T. Coyle, *Neurosci. Res.* **16**, 491 (1986).
- J. L. Arriza *et al.*, *J. Neurosci.* **14**, 5559 (1994).
- Rapid agonist applications were made as described (26). Recording pipettes contained either KSCN- or CsNO₃- based solutions (8), and extracellular solution consisted of 135 mM NaCl, 5.4 mM KCl, 5 mM Hepes, 1.8 mM CaCl₂, 1.3 mM MgCl₂, 100 μ M picrotoxin, 25 μ M NBQX, 25 μ M GYKI 52466, and 2.5 μ M CPP (pH 7.4).
- T. S. Otis, Y. C. Wu, L. O. Trussell, *J. Neurosci.* **16**, 1634 (1996).
- J. D. Clements, *Trends Neurosci.* **19**, 163 (1996).
- B. Barbour, B. U. Keller, I. Llano, A. Marty, *Neuron* **12**, 1331 (1994); M. Takahashi, Y. Kovalchuk, D. Attwell, *J. Neurosci.* **15**, 5693 (1995).
- N. Zerangue and M. P. Kavanaugh, *Nature* **383**, 634 (1996).
- Treatment of *Xenopus* oocytes was as described (5). Oocytes were injected with either human EAAT3 or EAAT4 mRNA and incubated 2 to 4 days in Ringer solution. Ten to 18 hours before recording, intracellular Cl⁻ was dialyzed by switching to Cl⁻-free Ringer solution containing 98 mM NaNO₃, 2 mM KNO₃, 1.8 mM Ca gluconate₂, 1 mM Mg gluconate₂, 5 mM Hepes (pH 7.5). For EAAT4, E_{rev} in this solution was -30 ± 2 mV (Fig. 3A, open triangles; $n = 8$). Neglecting the stoichiometrically coupled ionic current, which under these conditions is negligible for EAAT4 (5), the Nernst equation indicates that NO₃⁻ achieved a concentration of 31 mM in EAAT4-injected oocytes. [³H]-L-glutamate uptake was measured in oocytes voltage-clamped at -55 mV (5) in a modified solution containing identical concentrations of permeant anions as in the slice solution [119 mM NaCl, 2.5 mM KCl, 2.5 mM CaCl₂, 1.3 mM MgCl₂, and 5 mM Hepes (pH 7.5)].
- CF EPSCs (membrane potential $V_m = -28$ to -16 mV, mean $V_m = -23$ mV) and STCs ($V_m = -63$ to -52 mV, mean $V_m = -58$ mV) were recorded from 10 PCs with a pipette solution containing 95 mM Cs gluconate, 35 mM CsNO₃, 20 mM Hepes, 10 mM EGTA, and 1 mM MgCl₂ ($n = 9$). Mean EPSCs or STCs were integrated over 200 ms. Glutamate flux was estimated as the time integral of the STC divided by the mean charge/flux value for either EAAT3 or EAAT4 (16). These calculations assume the same proportion of anion current to glutamate flux throughout the STC as was measured at steady state in the oocyte experiments.
- Integration of an average of aEPSCs recorded at -70 to -80 mV yielded charge, Q_{aEPSC} , which was scaled (assuming aEPSC_{rev} = 0 mV and a linear relation between Q and V_m) to the appropriate V_m for the CF EPSC (mean $V_m = -28$ mV) in each of the 10 cells (17). Quantal content was then estimated as Q_{EPSC}/Q_{aEPSC} (range: 270 to 746, $n = 10$).
- N. Riveros, J. Fiedler, N. Lagos, C. Munoz, F. Orrego, *Brain Res.* **386**, 405 (1986); D. Bruns and R. Jahn, *Nature* **377**, 62 (1995).
- S. Mennerick and C. F. Zorumski, *Nature* **368**, 59 (1994).
- T. Muller and H. Kettenman, *Int. Rev. Neurobiol.* **38**, 341 (1995).
- N. C. Danbolt, G. Pines, B. I. Kanner, *Biochemistry* **29**, 6734 (1990); but see also E. A. Schwartz and M. Tachibana, *J. Physiol.* **426**, 43 (1990).
- J. I. Wadiche, J. L. Arriza, S. G. Amara, M. P. Kavanaugh, *Neuron* **14**, 1019 (1995).
- D. Bruns, F. Engbert, H. D. Lux, *ibid.* **10**, 559 (1993).
- C.-M. Tang, M. Dichter, M. Morad, *Science* **243**, 1474 (1989); D. J. A. Wyllie, S. F. Traynelis, S. G. Cull-Candy, *J. Physiol.* **463**, 193 (1993); S. F. Traynelis, R. A. Silver, S. G. Cull-Candy, *Neuron* **11**, 279 (1993).
- G. Tong and C. E. Jahr, *Neuron* **13**, 1195 (1994); J. S. Diamond and C. E. Jahr, *J. Neurosci.* **17**, 4672 (1997).
- We thank D. Bergles, J. Diamond, J. Dzubay, S. Eliasof, M. Jones, and J. Wadiche for helpful suggestions and comments on the manuscript; L. Klamo, S. Eliasof, J. Wadiche, and T. Zable for assistance with the oocyte experiments; and J. Diamond for the mEPSC analysis program. Supported by NS21419 (C.E.J.) and NS33270 (M.P.K.).

30 May 1997; accepted 23 July 1997

Dynamic Molecular Combing: Stretching the Whole Human Genome for High-Resolution Studies

Xavier Michalet,* Rosemary Ekong,* Françoise Fougerousse, Sophie Rousseaux,† Catherine Schurra, Nick Hornigold, Marjon van Slegtenhorst, Jonathan Wolfe, Sue Povey, Jacques S. Beckmann, Aaron Bensimon‡

DNA in amounts representative of hundreds of eukaryotic genomes was extended on silanized surfaces by dynamic molecular combing. The precise measurement of hybridized DNA probes was achieved directly without requiring normalization. This approach was validated with the high-resolution mapping of cosmid contigs on a yeast artificial chromosome (YAC) within yeast genomic DNA. It was extended to human genomic DNA for precise measurements ranging from 7 to 150 kilobases, of gaps within a contig, and of microdeletions in the tuberous sclerosis 2 gene on patients' DNA. The simplicity, reproducibility, and precision of this approach makes it a powerful tool for a variety of genomic studies.

Recent developments in whole genome sequencing projects have all emphasized the importance of refined physical mapping tools that bridge the gap between establishing genetic maps and sequence-ready clones (1). Conventional approaches such as sequenced tagged sites (STS), content ordering of large insert clones [YAC or bacterial artificial chromosomes (BAC)] (2), and restriction mapping of redundant sets of smaller clones (3), used for the building of physical maps, are tedious and time consuming. New techniques developed for the direct visualization of clones, such as optical mapping (4) or fiber-fluorescence in situ hybridization (FISH) approaches (5, 6),

have either attempted to speed up these physical mapping steps or resolve some ambiguities of restriction mapping. However, none of these can be used routinely or independently from other methods. Moreover, for the purpose of genetic disease screening and molecular diagnostics, there is a need for efficient techniques within the resolution range of a few kilobases (kb) to a few hundred kilobases, a challenge addressed neither by polymerase chain reaction (PCR)-based approaches (7) nor by cytogenetics techniques (8).

We describe an approach for physical mapping and molecular diagnostics directed to the aforementioned resolution range.

This approach combines major technical developments of the molecular combing phenomenon (9)—referred to as dynamic molecular combing (DMC)—with fluorescent hybridization. In this process, silanized cover slips (9–11) are dipped into a buffered solution containing genomic DNA (12) and, after 5 min of incubation, are pulled out with the mechanical device described in Fig. 1. During incubation, DNA molecules bind spontaneously to the cover slip surface by their extremities only. When the cover slips are pulled out of the solution at a constant vertical speed of 300 $\mu\text{m/s}$ (13), the meniscus (air solution–cover slip interface) exerts a constant restoring force on the immersed part of each anchored molecule, while their emerged part comes out with the surface (Fig. 1A). Because of their hydrophobicity, the silanized surfaces dry instantaneously as they are pulled out of the solution. This rapid process results in irreversibly fixed, parallel DNA fibers, aligned in a single direction all over the surface (Fig. 1B).

As in the previously described procedure (9), DMC results in constant stretching of DNA molecules. The measured stretching factor is uniform all over the surface, as verified by systematic measurements of λ -DNA molecules (48.5 kb) on test surfaces, yielding a factor of 2 kb/ μm . This stretching factor does not depend on the size of the DNA fragments (11, 14).

The major advantage of DMC is its ability to comb high concentrations of total genomic DNA in conditions preserving it from excessive shearing. This yields a very high density of fibers (which, for human samples, can reach up to hundreds of genomes per cover slip), with most DNA fragments longer than several hundred kilobases (Fig. 1B) (15). Moreover, a very large number of identical surfaces can be prepared from the same DNA solution.

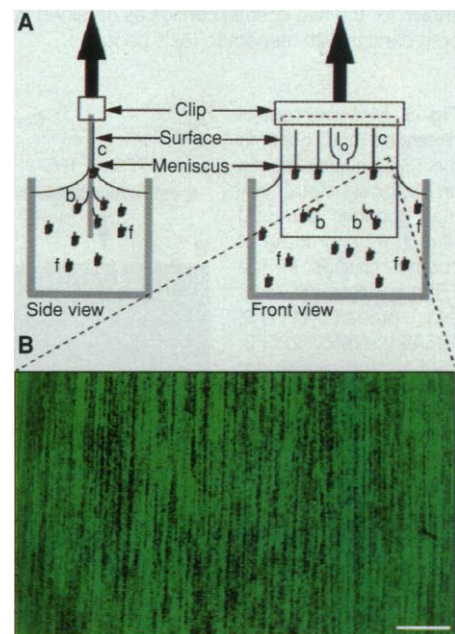
Fluorescent hybridization of DNA probes on combed DNA allows direct map-

ping of their respective positions along the fibers (16, 17). Because the density of fibers is high, scanning and recording of signals is fast, and numerous signals can be rapidly measured, allowing reliable distance measurements by statistical analysis, without reference to any other method or internal control. To calibrate and test the feasibility of this approach, we used it for the orientation and the refined physical mapping of the human calcium-activated neutral protease 3 gene (CAPN3 located on 15q15.2) contained in YAC 774G4. Mutations in this gene are responsible for the autosomal recessive limb-girdle muscular dystrophy type 2A (18). Cosmids of two contigs covering the gene region were hybridized; contig 1 has a known transcriptional orientation with respect to the centromere, whereas contig 2, which contains the CAPN3 gene, has not yet been orientated (Fig. 2). The orientation of contig 2 would be obtained from a sufficient number of independent measurements of distances between different pairs of cosmids belonging to both contigs.

Total yeast genomic DNA [12.6 megabases (Mb)] containing the YAC clone 774G4 (1.6 Mb) was obtained directly from yeast cells embedded in agarose blocks (12),

and no separation of the YAC was attempted. A solution of this DNA (7.5×10^6 genomes per milliliter) (19) was combed by DMC. Pairs of cosmids were then hybridized, and detected with a different fluorochrome [fluorescein isothiocyanate (FITC) (green) or Texas Red™ (red)] for each cosmid (17). Using only a fraction of a single 22 mm by 22 mm cover slip, tens of aligned pairs of red and green signals, as well as isolated signals, were systematically recorded. During the recording, no rejection of incomplete signals was made, in order to study the possibility of a purely statistical determination of real sizes and distances of signals. The analysis of the distributions of measurements, indeed, led to the assessment of an unambiguous size for both cosmids and for their distance, with a standard deviation of a few kilobases (20, 21). This strategy thus seems easily amenable to automation. Sizes of cosmids used in different hybridizations were reproducibly measured on different slides, and a further test of the stretching uniformity was obtained from redundant measurements of a few long distances (21, 22). This consistency allows a confident use of a constant stretching factor of 2 kb/ μm to translate these measurements into kilobases, without requiring a probe of

Fig. 1. Dynamic molecular combing of total genomic DNA. The technique involves four steps: (i) preparation of suitable surfaces coated with trichlorosilane (9–11), (ii) preparation of a DNA solution from DNA embedded in low-melting agarose blocks (12), (iii) incubation of surfaces in the solution for 5 min, and (iv) extraction of the surfaces out of the solution at a constant speed (300 $\mu\text{m/s}$) (13). **(A)** Steps (iii) and (iv) are performed in a Teflon™ reservoir, using a molecular combing apparatus consisting of a vertically moving clip holding one or more cover slips. We used silanized 22 mm by 22 mm cover slips, which were dipped vertically at a constant speed (300 $\mu\text{m/s}$) into a 4-ml Teflon reservoir containing either an $\sim 0.25 \mu\text{g/ml}$ solution of total yeast genomic DNA in 50 mM MES (pH 5.5) or an $\sim 1.5 \mu\text{g/ml}$ solution of total human genomic DNA in 150 mM MES (pH 5.5) (12). Freely floating molecules (f) randomly bind to the surface by their extremities. For clarity, the random coil of the bound molecule (b) is represented as exaggeratedly distant from the anchoring point. The cover slip area below the meniscus line is immersed. As the cover slip is pulled out of the solution after a 5-min incubation period, the anchoring points move upward with the surface. The fixed, horizontal meniscus exerts a localized, constant, and downward vertical force on the coil of the molecules, which are thus progressively unwound. The unwound part is stretched and irreversibly fixed on the dry part of the surface (c). Some loops are observed (lo) when DNA fragments are bound at both extremities, as described (9). **(B)** One field of view (200 μm by 120 μm) is shown of combed human genomic DNA, observed with an epifluorescence microscope (Axioskop, Zeiss, Plan Neofluar 40 \times objective) with an attached intensified video camera (SIT 68, Dage-MTI). Most of the DNA strands span several fields of view, corresponding to hundreds of micrometers (1 $\mu\text{m} \equiv 2 \text{ kb}$). The density of fibers shown is close to the maximum for optimal combing. Spherical deformations due to the intensified camera were corrected and image was contrast-enhanced with a homemade computer software. Differences in fluorescence intensity can be attributed to local bundling of a few DNA molecules. Bar, 25 μm .



X. Michalet, C. Schurra, A. Bensimon, Laboratoire de Biophysique de l'ADN, Département des Biotechnologies, Institut Pasteur, 25 rue du Dr. Roux, 75724 Paris Cedex 15, France.

R. Ekong, S. Rousseaux, S. Povey, MRC Human Biochemical Genetics Unit, University College London, 4 Stephenson Way, London NW1 2HE, UK.

F. Fougerousse and J. S. Beckmann, URA 1922, Génomique, 1 rue de l'Internationale, Boîte Postale 60, 91002 Evry, France.

N. Hornigold and J. Wolfe, The Galton Laboratory, Department of Biology, University College London, 4 Stephenson Way, London NW1 2HE, UK.

M. van Slegtenhorst, Department of Clinical Genetics, Erasmus University, Dr. Molewaterplein 50, NL-3015, GE Rotterdam, Netherlands.

*These authors contributed equally to this work.

†Present address: INSERM U309, Institut Albert Bonniot, 39706 La Tronche Cedex, France.

‡To whom correspondence should be addressed. E-mail: abensim@pasteur.fr

known size as an internal control, contrary to previously published fiber-FISH methods (5, 6). As a result, we obtained a precise physical map spanning more than 200 kb on the YAC covering the region (Fig. 2), with the determination of the gap size

(44.6 ± 5.8 kb) between both contigs (21, 22). This unambiguous orientation of the contigs showed a centromere-to-telomere transcriptional polarity of CAPN3.

Because the high density of signals allows the fast recording of enough measure-

ments to obtain precise, statistically significant sizes and distances, this approach appears to be a powerful, autonomous tool for the construction of high-resolution maps, including sequence-ready maps over distances up to a few hundred kilobases (23), starting, for instance, from groups of clones roughly ordered by STSs content. Moreover, this approach has advantages over restriction mapping in that it measures gap sizes and is free of ambiguities that can result from unresolved fragments.

However, the use of cloned DNA in human genome studies, especially of YACs, is often impaired by rearrangements. Furthermore, even an unrearranged clone reflects the organization of one chromosome only. Extension of the DMC approach to human genomic DNA was thus a critical challenge, not only to avoid problems with large, unstable clones, but also to address diagnostic questions directly. However, because the human genome [~ 3 gigabases (Gb)] is much larger than any cloned DNA (with the largest host genome size of 12.6 Mb for YAC), higher concentrations of DNA have to be used, and larger parts of a slide have to be scanned to obtain statistically significant results.

We have first confirmed the feasibility of genomic studies of combed total human genomic DNA on the tuberous sclerosis 1 (TSC1) gene region. Tuberous sclerosis (TSC) is an autosomal dominant heterogeneous disease, characterized by the development of benign growths in several organs, and has two known genetic loci, TSC1 and TSC2 (24). Although TSC2 was cloned in 1993 (25), TSC1 on chromosome 9q34 has only very recently been identified (25). During the positional cloning of TSC1, the construction of a cosmid contig gave an unambiguous order of cosmids (26). However, two gaps remained for which no accurate distances could be obtained by standard fiber-FISH methods (6) because of the paucity of hybridization signals, attributed to the scarcity of DNA fibers and variable degrees of stretching.

Hence, the gap sizes in the TSC1 cosmid contig (Fig. 3A) were determined by hybridizing pairs of cosmid probes on combed human genomic DNA (12), detected with different fluorochromes (17). Measurements of up to 80 intact pairs of red and green signals were performed on a single slide (27). The uniformity of stretching was apparent from the similar lengths of hybridization signals (Fig. 3B) and was confirmed by the standard deviations of, at most, a few micrometers on the measured distances. This uniformity and the validation by the previous yeast experiments allowed direct determination of gap sizes in kilobases (28). An independent measurement of one of the

Fig. 2. (A) STSs map of some cosmids of the two contigs covering the CAPN3 gene region (contig 1, red; contig 2, green). STSs used for contig orientation are represented as vertical bars separated by an arbitrary distance (18). Contig 1 has a known chromosomal orientation. The CAPN3 gene exons are contained in 1F11 and 1G3 (18). The vertical dotted line indicates a gap of unknown size. (B) Shown are names of cosmid pairs used in each hybridization experiment and manually aligned, representative signals for each pair of hybridized cosmids illustrating the high-resolution map obtained over a distance of 200 kb. Images were captured with a charge-coupled device (CCD) camera (Photometrics) mounted on an epifluorescence microscope (Axioskop, Zeiss), with a 100 \times or 63 \times objective. A homemade software was used for the precise measurement of sizes and for their statistical analysis (21). The size of the gap is 44.6 ± 5.8 kb (21, 22). Bar, 10 μ m = 20 kb. (C) Final orientation is shown for the two cosmid contigs as obtained from DMC experiments. A reversal of the orientation of both contigs with respect to (A) is deduced.

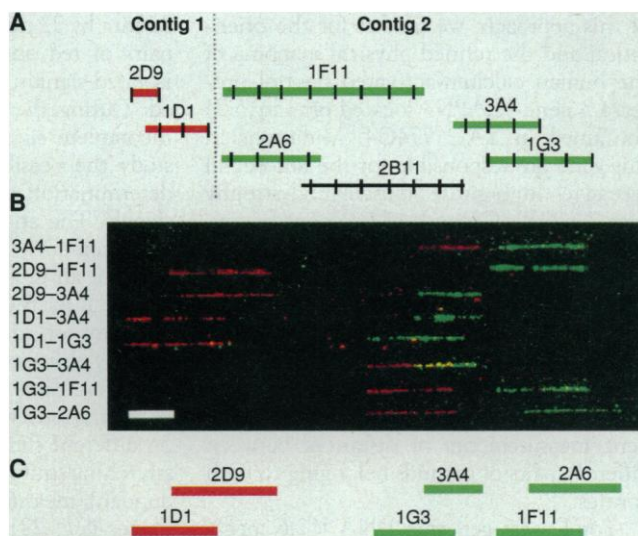
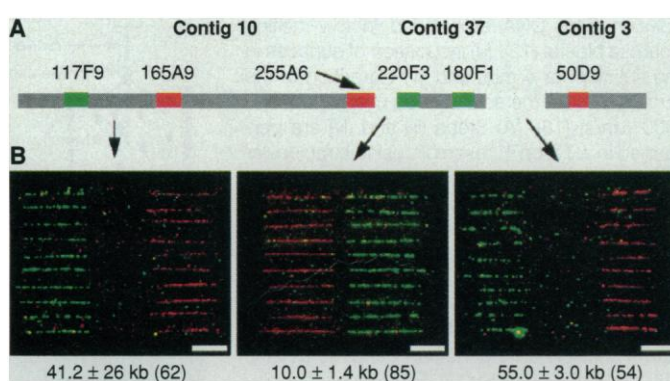


Fig. 3. Measurement of distances and gaps in the TSC1 cosmid contig on combed total human genomic DNA. (A) Sketch (not to scale) of cosmid contigs in the TSC1 gene region. Cosmid probes (117F9, 165A9, 255A6, 220F3, 180F1, and 50D9) for determining gap sizes were all obtained from a chromosome-9-specific library, LL09NC01*P, and were all within the

TSC1 gene region on 9q34 between the markers D9S149 and D9S114 (34). The first two cosmids (117F9 and 165A9) within contig 10 were used as controls. Cosmids 255A6 (contig 10) and 220F3 (contig 37) are at the end of their respective contigs and border a gap subsequently bridged by two PACs (213M24 and 145N8) (34). Cosmid 180F1 (contig 37) and 50D9 (contig 3) are not at the ends of their respective contigs, and the measured distance thus only sets up an upper limit for the gap size, which has been estimated with the help of PFGE to be ~ 20 kb. Subsequent DMC measurements with cosmid probes (250D5 and 251C9) bordering this gap have given a distance of ~ 23 kb (35) (B) Montage of 10 representative pairs of signals on each slide of combed total human genomic DNA shows distances between cosmids in the TSC1 contigs. Bars, 10 μ m = 20 kb. The images are exactly as observed under the microscope and captured on the CCD camera, after standard contrast enhancement. Each montage was assembled from individual pairs of signals that had been captured in a single field of view. No normalizations of the images have been performed, showing the uniformity of stretching. Distances are displayed together with the corresponding standard deviation of the measurements and the number of measurements retained for the final computations (in brackets). The measurements for cosmids 117F9 and 165A9 (41.2 ± 2.6 kb) are in good agreement with measurements from Eco RI mapping (39 kb; M. van Slegtenhorst, data not shown), considering the possible uncertainties of restriction mapping due to overlapping bands.



gaps by Eco RI restriction mapping gave a size that was in very good agreement with the result from DMC (Fig. 3).

The reliability of the DMC approach on the human genome opens the way for a wide range of genetic studies not accessible by other techniques, for instance, the detection and precise measurement of micro-rearrangements (such as microdeletions in disease genes) which can be arduous and time consuming. Conventional approaches used for detecting loss or gain of DNA sequences do not provide accurate information on sizes of missing or additional sequences unless detection of abnormal results is followed by sequencing (29). Mutations may sometimes be missed altogether because of the resolution of the methods used in searching for them. Estimates for sizes of deletions can be obtained by pulsed-field gel electrophoresis (PFGE), but the resolution of this method prevents the detection and measurement of deletions below 10 kb. Added limitations include the determination of PFGE parameters required for adequate separation of DNA fragments which can be problematic and lengthy.

As a model example, we chose to measure the sizes of known microdeletions involving the TSC2 gene, the other tuberous sclerosis gene, located on 16p13.3 (25). For the TSC2 patients studied here, the sizes of deletions, as previously estimated by PFGE, range from 46 to 160 kb (25, 30).

DNA was prepared (12) from peripheral blood lymphocytes from a normal subject and from three patients carrying deletions involving the TSC2 gene. Each sample was combed separately. Two cosmids bordering the gene region (CBFS1 and GGG4A) were hybridized onto each DNA sample and detected with different fluorochromes (17). For the healthy subject, one single distance of 147 ± 4.4 kb between the two closest extremities of the cosmids was measured, which corresponds to two identical alleles (Fig. 4). This result is in good agreement with the previous PFGE measurement of 150 kb (31). Hybridizations of these cosmids on DNA from each TSC2 patient yielded two distances, corresponding respectively to the normal allele (~ 150 kb) and to the deleted one (Fig. 4 and Table 1). The distance between the two cosmids on the normal allele of all patients agreed with that measured for both alleles of the healthy individual. This shows the reproducibility of the approach used on different DNA samples prepared on different days and combed onto different batches of silanized surfaces. One of the cosmid signals (CBFS1) was partially deleted on the abnormal allele of two patients (WS-212 and WS-9), yet the size of these partial dele-

tions was precisely determined, increasing the resolution of the technique for deletion measurement down to a few kilobases.

In summary, the DMC approach described here is a simple method for stretching total genomic DNA from various kinds of cellular material, like blood lymphocytes, lymphoblastoid cell lines, or amniotic cells (32), provided their DNA has been preserved from degradation and that cells can be embedded in agarose blocks (12). It allows precise and quantitative measurements of the sizes of hybridized DNA clones and distances between them, at a resolution ranging from a few kilobases up to a few

hundred kilobases for both, without requiring normalization by other methods. We have applied DMC to the refinement of a sequence-ready cosmid map, measurement of gaps between contigs on total human genomic DNA, and the measurement of microdeletions on patients' DNA. This approach is of interest not only in genomics, for instance in genome sequencing projects that require validation of sequence-ready maps, but also in diagnostics, where new tools for well-characterized diseases are needed. DMC can be used to check the integrity and stability of large DNA clones such as the human artificial chromosomes

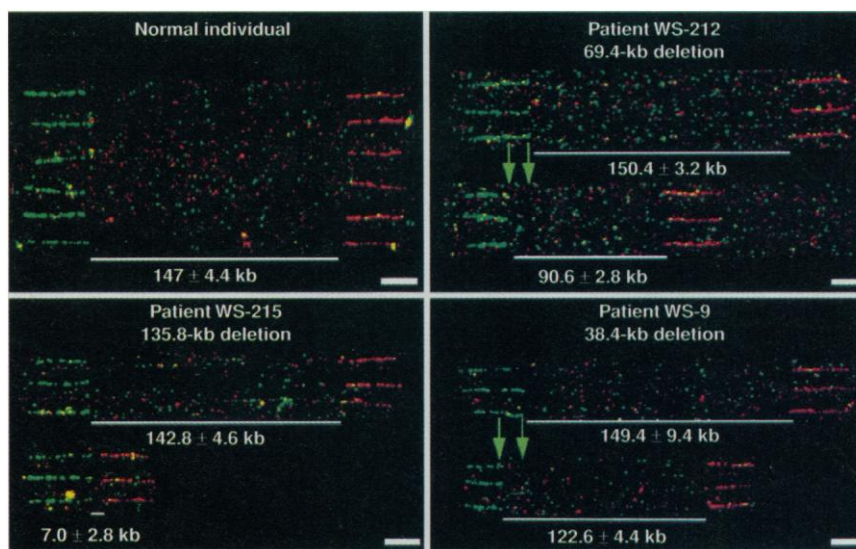


Fig. 4. Measurement of deletions involving the TSC2 gene region in affected patients. Cosmids CBFS1 (at the distal end of TSC2) and GGG4A (at the proximal end) were hybridized onto combed total genomic DNA slides and detected with two different fluorochromes [CBFS1 (green) and GGG4A (red)] (17). For each experiment, a montage of six representative pairs of signals is shown, without any normalization. The pictures were assembled as described in Fig. 3B. The top three pairs of signals from each patients' slide (WS-212, WS-9, WS-215) represent the normal allele, whereas the lower three show the allele with the deletion. In two patients (WS-212 and WS-9), one cosmid signal was partially deleted, and the deleted part of the sequence is indicated by two green arrows. See Table 1 for details. Bars, $10 \mu\text{m} = 20$ kb.

Table 1. Comparison of distance measurements (in kilobases), using DMC and PFGE. Dynamic molecular combing of human genomic DNA: for the normal subject, one single distance was measured, because both alleles are normal in the region bordered by the two cosmids. For TSC2 patients, two distances were measured, corresponding to the normal allele and to the deleted one. Measured distances are displayed with their SDs and the number of measurements taken into account for the calculations (in brackets). The distances corresponding to the normal allele (first column) for four different samples shows the uniformity of stretching obtained even for long-distance measurements. The total size of the deletion is derived from results of the first columns: total deletion = distance on normal allele - distance on deleted allele + cosmid deletion. PFGE: approximate sizes of deletions for the three patients were determined by PFGE (24, 29). Cosmids CBFS1 and GGG4A border the TSC2 gene region and their distance has previously been estimated on normal DNA to be 150 kb by PFGE (31).

DNA origin	Distance on normal allele	Deletion in CBFS1 cosmid	Distance on deleted allele	Total deletion (DMC)	Total deletion (PFGE)
Normal	147 ± 4.4 [11]	0	0	0	0
WS-212	150.4 ± 3.2 [36]	9.6 ± 1.8 [20]	90.6 ± 2.8 [18]	69.4 ± 4.6	75*
WS-9	149.4 ± 9.4 [18]	11.6 ± 2.6 [21]	122.6 ± 4.4 [35]	38.4 ± 10.7	46†
WS-215	142.8 ± 4.6 [8]	0	7.0 ± 2.8 [41]	135.8 ± 5.4	160*

*Reference 29. †Reference 24.

or chromosomes of human-mouse hybrids (33), visualize and measure intragenic rearrangements, map translocation breakpoints in disease loci, assist in the identification of disease genes, and compare maps between species, which should lead to insights in the evolutionary process.

REFERENCES AND NOTES

- R. D. Fleischmann *et al.*, *Science* **269**, 496 (1995); A. Goffeau *et al.*, *ibid.* **274**, 546 (1996); R. A. Gibbs, *Nature Genet.* **11**, 121 (1995). J. L. Weber and E. W. Myers, *Genome Res.* **7**, 401 (1997). P. Green, *ibid.*, p. 410.
- I. M. Chumakov *et al.*, *Nature* **373** (suppl.), 175 (1995); C. Boysen, M. I. Simon, L. Hood, *Genome Res.* **7**, 330 (1997).
- K. E. Davies, Ed., *Genome Analysis: A Practical Approach* (IRL, Oxford, UK, 1988).
- D. C. Schwartz *et al.*, *Science* **262**, 110 (1994); X. Meng, K. Benson, K. Chada, E. J. Huff, D. C. Schwartz, *Nature Genet.* **9**, 432 (1995); H. Yokota *et al.*, *Nucleic Acids Res.* **22**, 1064 (1997).
- J. Wiegant *et al.*, *Hum. Mol. Genet.* **1**, 587 (1992); T. Haaf and D. C. Ward, *ibid.* **3**, 697 (1994); R. J. Florjanc *et al.*, *ibid.* **5**, 831 (1995); I. Parra, B. Windle, *Nature Genet.* **5**, 17 (1993).
- H. Fidlerova, G. Senger, M. Kost, P. Sanseau, D. Sheer, *Cytogenet. Cell Genet.* **65**, 203 (1994); G. Senger *et al.*, *Hum. Mol. Genet.* **3**, 1275 (1994); M. Heiskanen *et al.*, *Genomics* **30**, 31 (1995).
- B. Pertl *et al.*, *Lancet* **343**, 1197 (1994); M.-C. Cheung, J. D. Goldberg, Y. W. Kan, *Nature Genet.* **14**, 264 (1996).
- J. K. Blacato *et al.*, *J. Reprod. Med.* **40**, 537 (1995).
- A. Bensimon *et al.*, *Science* **265**, 2096 (1994); D. Bensimon, A. J. Simon, V. Croquette, A. Bensimon, *Phys. Rev. Lett.* **76**, 4754 (1995).
- X. Michalet and A. Bensimon, data not shown.
- J.-F. Allemand, D. Bensimon, L. Jullien, A. Bensimon, V. Croquette, *Biophys. J.*, in press.
- Preparation of genomic DNA and combing was as follows. Yeast DNA: Yeast DNA containing YAC 774G4 (1.6 Mb) was prepared from 50-ml yeast cultures [I. H. Evans, Ed., *Yeast Protocols: Methods in Cell and Molecular Biology*, vol. 53 of *Methods in Molecular Biology* (Humana, Totowa, NJ, 1996), p. 71]. Yeast cells were put in 100 μ l of 0.5% (final concentration) low-melting point agarose blocks (1 μ g per block), using standard PFGE block preparation protocol (3). Total human genomic DNA: DNA blocks were prepared from peripheral blood lymphocytes from a normal subject or lymphoblastoid cell lines from patients carrying deletions involving the TSC2 gene. Peripheral blood lymphocytes were separated from fresh whole blood with lymphocyte separation medium (Flow Labs); this step was not required for lymphoblastoid cells. After washing in phosphate-buffered saline (PBS), cells were resuspended at a concentration of 2×10^7 cells/ml, mixed with an equal volume of 1% low-melting point agarose, and immediately poured into 100- μ l molds. Each block contained 10^6 cells, equivalent to 6.6 μ g of genomic DNA for diploid cells (3). PFGE blocks were then prepared as described (3) with the following modifications: ESP contained 2 mg/ml proteinase K, 0.5 M EDTA (pH 8), and 1% L-sarcosine, and blocks were stored in 0.5 M EDTA (pH 8) at 4°C. Combing: Before use, blocks were washed in 15 ml of TE buffer [10 mM Tris/1 mM EDTA (pH 8)] for at least 2 hours. Each agarose block was stained with the fluorescent dye YOYO-1 (0.33 nmol per microgram of DNA; Molecular Probes) in 100 μ l of $T_{40}E_2$ [40 mM Tris/2 mM EDTA (pH 8)] in 2-ml Eppendorf tubes for 1 hour at room temperature (RT). After staining, the supernatant was discarded and each agarose block was melted for 20 min in 500 μ l of TE buffer at 68°C, then digested for 2 hours or overnight at 40°C with 2 U of β -agarase I in $1 \times$ NEB agarase buffer (New England Biolabs). Dilution of the DNA (yeast, 0.25 μ g/ml; human, 1.5 μ g/ml) in MES (pH 5.5) [yeast, 50 mM; human, 150 mM (final concentrations)] was performed very carefully in 15-ml round-bottomed tubes (Falcon) in order to avoid breakage of the DNA strands. Because of high DNA concentrations in the human DNA preparations, suspension of the DNA had to be aided by heating the solution to 75°C for 30 min, then cooling to RT before transfer to a reservoir. The DNA solution was poured into a Teflon™ reservoir of appropriate size. Up to three silanized 22 mm by 22 mm cover slips could be introduced in a 4-ml reservoir. The DNA solution can be stored at 4°C for several weeks. Combed DNA cover slips (see text and Fig. 1) were examined with an inverted epifluorescence microscope (Axiovert 135, Zeiss) equipped with filter for green emission (XF 22, Omega Optical). Surfaces with DNA density as shown in Fig. 1 were used in fluorescent hybridization experiments. Before use, DNA cover slips were dried at 60°C overnight, mounted on microscope slides with cyanoacrylate glue, and used immediately or stored (-20°C) in plastic slide holders. DNA cover slips have been stored at RT for up to 6 months before use in FISH experiments without any deterioration in the quality of the hybridization or quantity of signals (34).
- Shorter incubation times (30 s) of the slides in the DNA solution have also been used successfully, implying that the kinetics of DNA binding is probably very fast, with a rapid saturation of all accessible binding sites. The quality of combing does not depend on the speed at which cover slips are pulled out of the DNA solution [speeds of up to 500 μ m/s have been used (10)].
- This parameter is constant for each batch of treated surfaces. For unexplained reasons, a few batches with a stretching factor of 2.3 kb/ μ m have sometimes also been observed. Hence, systematic measurements of λ -DNA molecules were performed on a few surfaces per batch (each batch containing 72 surfaces). Surface treatment inhomogeneities on each cover slip may occur and lead to local variations in the surface density of combed molecules, or in the stretching factor. However, these inhomogeneities have no effect on the final results obtained on a large number of measurements, as shown by their small standard deviation (see text). Residual surface defects may also result in transient pinning of the meniscus, leading to a local deformation of the normally straight interface. It can be detected as a local departure from parallelism, but has no effect on the stretching factor. The validity of this factor for a wide range of DNA sizes was shown by measurement of molecules ranging from ~50 kb to ~250 kb (11) and by redundant measurements of cosmid distances (21).
- The number of combed genomes is estimated from the mean DNA length per field of view, the theoretical length of a combed genome, and the number of fields of view per cover slip. The size distribution of the fragments cannot be systematically measured because the extension of fibers over several fields of view and their density render it a cumbersome analysis. The mean length given here is a qualitative order of magnitude. Among these long fibers, a significant proportion of fragments have lengths over several megabases.
- H.-U. G. Weier *et al.*, *Hum. Mol. Genet.* **10**, 1903 (1995).
- Probe labeling: all probes consisted of genomic DNA cloned in cosmids. Cosmids were grown and DNA extracted with a scaled-up alkaline lysis method (3). Each probe (1 μ g) was labeled by random priming with either biotin-14-deoxycytosine triphosphate (Bioprime kit, Gibco-BRL) or digoxigenin-11-deoxyuridine triphosphate (DIG, Boehringer) according to manufacturer's instructions. Ethanol-precipitated probes were resuspended in 50 μ l of 10 mM Tris/1 mM EDTA (pH 8) and stored at -20°C. Concentrations were estimated by densitometry on a 0.6% agarose gel. Probes labeled by nick-translation have also been used. We again ethanol precipitated 500 to 600 ng of each labeled probe in the presence of 5 \times excess human COT-1 DNA (except when hybridizing on yeast DNA, for which no COT-1 was used) and 20 μ g of herring sperm DNA at -70°C for 1 hour. After centrifugation, the pellet was dried for 10 min, then resuspended in 10 μ l of hybridization mixture [50% formamide, 10% dextran sulfate, 2 \times saline sodium citrate (SSC), and 1% Tween-20]. Resuspended probes were denatured (5 min in boiling water), snap-cooled, and left on ice until needed. Slides: Combed DNA cover slips mounted on microscope slides were equilibrated to RT, dehydrated through ethanol series (70%, 90%, 100%) three times of 3 min each, air-dried, denatured in 50% formamide/2 \times SSC (pH 7.0) at 75°C for 2 min, then quenched in ice-cold ethanol series and air dried. Hybridization: Denatured probes were incubated with combed DNA at 37°C under an ordinary glass cover slip, with the edges sealed with rubber cement, for at least 16 hours. Detection: All slides were washed at RT on a shaker as follows: three washes of 5 min in 50% formamide/2 \times SSC (pH 7) and three washes of 5 min in 2 \times SSC. We applied 50 μ l of 1.5% blocking solution (Boehringer) on each DNA cover slip and incubated them at 37°C for 30 min in a moist chamber. Biotinylated and DIG-labeled probes were detected with Texas red and FITC, respectively, using five successive layers of antibodies as follows: (i) avidin-Texas red 1/50 (Vector Labs) + anti-DIG-FITC (mouse) 1/50 (Jackson ImmunoResearch Labs); (ii) biotinylated anti-avidin 1/100 (Vector Labs) + anti-mouse-FITC (donkey) 1/50 (Jackson ImmunoResearch); (iii) avidin-Texas red 1/50 + anti-rabbit (mouse) 1/50 (Jackson ImmunoResearch); (iv) biotinylated anti-avidin 1/100 + F1 (anti-FITC; Camburg) 1/400; and (v) avidin-Texas red 1/50 + F2 (anti-FITC; Camburg) 1/100. The last two layers were necessary to increase the intensity of the signals. All antibody incubations were at 37°C; the first three were for 30 min each and the last two for 20 min each. All antibody washes were for three times of 5 min at RT using 4 \times SSC/0.05% Tween-20. A final wash in PBS was performed, and the slides were drained and mounted in Vectashield (Vector Labs) without counterstain.
- F. Fougerousse *et al.*, *Hum. Mol. Genet.* **2**, 285 (1994); I. Richard, C. Roudaut, F. Fougerousse, N. Chiannilkuchai, J. S. Beckmann, *Mamm. Genome* **6**, 754 (1995); I. Richard *et al.*, *Cell* **81**, 27 (1995).
- At this concentration, the DNA solution behaves like a polymer melt, and no fast drying can be expected if a drop of solution is deposited on a cover slip as described (9, 16). Moreover, the unbound molecules entangled in the polymer mesh of other molecules are forced to dry on the surface, which results in uncombed patches of DNA. Manipulation of the DNA would also contribute to intense shearing, which is eliminated by the use of a fixed reservoir and the molecular combing apparatus described in Fig. 1A.
- For small distances between two probes (<30 kb), >50% of the pairs of aligned red and green cosmid signals were complete. Inversely, in most pairs of cosmids separated by longer distances, one or both cosmids were detected as incomplete signals (21). This is due to an increased probability of finding a broken DNA fragment in the region studied (and hence, partial hybridization signals). In such cases, the size of each cosmid was reliably determined because we also included measurements of isolated, complete cosmid signals in our analysis.
- X. Michalet *et al.*, in preparation.
- Redundant measurements consist of measuring the distance between cosmid A and B, the distance between B and C, and the distance between A and C in three different hybridization assays. Any stretching inhomogeneity would give different results for the distance between A and C, as obtained from the sum of the first two hybridizations and from the direct measurement of the third one. A perfect agreement was observed in all independent tests (over a 200-kb region), which allowed us to convert mean sizes measured in micrometers to sizes measured in kilobases, without needing to refer to an internal control. Direct measurements have standard deviations of 6 to 11%. The gap size was measured indirectly from two measurements, which led to a larger standard deviation (21).
- The maximum extent over which this approach can

- be used is restricted mainly by the size of the microscope field of view (which can be increased using smaller magnification objectives at the expense of visibility of fluorescent signals) and by the difficulty to assess whether two apparently distant and aligned signals belong to the same fiber or not, setting a practical distance limit of a few hundred kilobases [400 kb, 40 \times objective (27)]. Detection of the underlying DNA fiber with another fluorochrome (16) does not resolve this ambiguity when the density of combed fibers is too high, because of the possible confusion between close fibers (27). Hybridization of several probes together, detected with multicolor fluorescent systems, would decrease the number of hybridizations and the scanning time necessary for the construction of large high-resolution physical maps, contrary to optical mapping techniques that require one experiment per clone.
24. S. Povey *et al.*, *Ann. Hum. Genet.* **58**, 107 (1994).
 25. The European Chromosome 16 Tuberous Sclerosis Consortium, *Cell* **75**, 1305 (1993); M. van Sleghenhorst *et al.*, *Science* **277**, 805 (1997).
 26. J. Nahmias *et al.*, *Eur. J. Hum. Genet.* **3**, 65 (1995); M. van Sleghenhorst *et al.*, *ibid.*, p. 78.
 27. This yield of about 50 to 100 pairs of hybridized cosmids is in agreement with the rough estimate of DNA density of, at most, a few hundred combed genomes per slide (14). The total number of genomes as estimated, also including the incomplete and isolated signals, is indeed much closer to the one estimated from combing density, thus showing a satisfactory hybridization efficiency (R. Ekong and X. Michalet, data not shown; J. Herrick *et al.*, in preparation).
 28. In both experiments, comparison of measurements done on different slides (slides prepared

- on different days but from the same DNA solution or from different DNA agarose blocks using either the same or different batches of silanized cover slips) gave similar results.
29. A. J. Green, M. Smith, J. R. W. Yates, *Nature Genet.* **6**, 193 (1994); D. Niederacher *et al.*, *Genes Chromosomes Cancer* **18**, 181 (1997); M. Lastowska *et al.*, *ibid.* **18**, 162 (1997); A. Kallioniemi *et al.*, *Science* **258**, 818 (1992); E. Schröck *et al.*, *ibid.* **273**, 494 (1996); M. R. Speicher, S. G. Ballard, D. C. Ward, *Nature Genet.* **12**, 368 (1996); T. Veldman, C. Vignon, E. Schröck, J. D. Rowley, T. Ried, *ibid.* **15**, 406 (1997).
 30. P. T. Brook-Carter *et al.*, *Nature Genet.* **8**, 328 (1994).
 31. J. Sampson, personal communication.
 32. A. Bensimon, data not shown.
 33. J. J. Harrington, G. van Bokkelen, R. W. Mays, K. Gustashaw, H. F. Willard, *Nature Genet.* **15**, 345 (1997); K. Tomizuka *et al.*, *ibid.* **16**, 133 (1997).
 34. N. Hornigold *et al.*, *Genomics* **41**, 385 (1997).
 35. R. Ekong, data not shown.
 36. X.M. benefited from a Pasteur-Weizmann grant, S.R. from a Wellcome Trust grant, and M.V.S. from support by the Dutch Organisation for Scientific Research. We thank A. Chiffaudel for technical help in the development of the combing apparatus, J. Sampson and P. Harris for providing us with TSC2 probes and patient cell lines, and J. Nahmias for unpublished data on the TSC1 contig. Supported in part by the Association Française contre les Myopathies. Dedicated to A. Ullmann for constant support throughout this project.

11 March 1997; accepted 3 July 1997

Conditional Mutator Phenotypes in hMSH2-Deficient Tumor Cell Lines

Burt Richards, Hong Zhang, Geraldine Phear, Mark Meuth*

Two human tumor cell lines that are deficient in the mismatch repair protein hMSH2 show little or no increase in mutation rate relative to that of a mismatch repair-proficient cell line when the cells are maintained in culture conditions allowing rapid growth. However, mutations accumulate at a high rate in these cells when they are maintained at high density. Thus the mutator phenotype of some mismatch repair-deficient cell lines is conditional and strongly depends on growth conditions. These observations have implications for tumor development because they suggest that mutations may accumulate in tumor cells when growth is limited.

The autosomal dominant syndrome of hereditary nonpolyposis colon cancer (HNPCC) is characterized by early onset of colon tumors as well as cancers of the endometrium, stomach, upper urinary tract, small intestine, and ovary. Mutations in two human homologs of the *Escherichia coli* mismatch repair genes *MutS* and *MutL* (*hMSH2* and *hMLH1*) are found in the great majority of HNPCC patients (1). Less frequent germline mutations of another *MutL* homolog (*hPMS2*) are also associated with this disease (2). HNPCC patients in-

herit a mutant allele of a mismatch repair gene (3), and the second wild-type allele is mutated or lost as an early event in tumor development (3, 4). This second event renders cells mismatch repair-deficient (5, 6), presumably leading to a mutator phenotype that drives the accumulation of mutations required for tumor development (7). Two other genes encoding homologs of the *E. coli* *MutS* gene (*hMSH3* and *hMSH6*) appear to be involved in the repair of some types of DNA replication errors or damage (8). A variety of in vitro assays indicate that heterodimers formed between these proteins and hMSH2 exhibit considerable specificity in the types of errors they recognize and bind. Thus, hMSH2 may play a central role in recognition of DNA replica-

tion errors while hMSH3 and hMSH6 modify the specificity of this recognition (8).

To examine the consequences of hMSH2 deficiency in human tumor cells, we measured mutation rates in two tumor cell lines with *hMSH2* mutations: SK-UT-1, which was derived from a uterine tumor; and 2774, which originated from an ovarian tumor (6, 9–11). SK-UT-1 has a 2-base pair (bp) deletion in exon 10 of the *hMSH2* coding sequence that results in a truncation (9); and 2774 has a base substitution in exon 14, resulting in a missense mutation (Arg \rightarrow Pro) (10). SK-UT-1 has no detectable hMSH2 protein, whereas 2774 retains a full-length mutant protein (12). The levels of hMLH1 and hPMS2 in these cell lines are similar to those in repair-proficient cell lines. Surprisingly, mutation rates of growing 2774 and SK-UT-1 cells at the X-linked locus encoding the purine salvage enzyme hypoxanthine guanine phosphoribosyl transferase (*HPRT*) (Table 1) were lower than that measured for the mismatch repair-proficient SV40-transformed fibroblast line MRC-5 (rate = 1.4×10^{-7} mutations per cell per generation). This contrasts with the 130- to 190-fold increase in mutation rate found in tumor cell lines deficient in other mismatch repair components (Table 2). Other laboratories have reported difficulties in isolating *HPRT* mutants from hMSH2-deficient cell lines (13), although increased mutation rates have been measured in the hMSH2-deficient LoVo cell line (14, 15). To test the possibility that the low *HPRT* mutation rate in the hMSH2-deficient cells is due to the presence of multiple active X chromosomes (16), we measured the rate of mutation to ouabain resistance (*Oua^R*). Because these mutations act dominantly, they are not obscured in polyploid cells (17). However, even at this locus there was no change in mutation rate for cell line 2774 relative to that in mismatch repair-proficient MRC-5, whereas that in SK-UT-1 was elevated 7.1-fold (18). Thus, these data indicate that the two hMSH2-deficient tumor cell lines develop a weaker mutator phenotype than lines deficient in other mismatch repair genes.

To determine whether mutation rates increased in these hMSH2-deficient cells under less optimal culture conditions, we examined *HPRT* and *Oua^R* mutant frequencies in 2774 and SK-UT-1 cells that had been maintained for 2 weeks in a high-density growth-limited state. For 2774 cells, the *HPRT* mutant frequency of replicas maintained at high density was 7900-fold higher and the frequency of *Oua^R* mutants was >67-fold higher relative to those of replica cultures kept under optimal growth conditions (Table 1). SK-UT-1 cells main-

Departments of Oncological Sciences and Radiation Oncology, Eccles Institute of Human Genetics, University of Utah, Salt Lake City, UT, 84112, USA.

*To whom correspondence should be addressed. E-mail: mark.meuth@genetics.utah.edu